Temperature and Molecular Weight Variation of Gaseous Injection into a Supersonic Stream," AIAA Paper 69-1, New York, 1969.

[10] Dowdy, M. W. and Newton, J. F., Jr., "Investigation of Liquid and Gaseous Secondary Injection Phenomena on a Flat Plate with M = 2.01 to M = 4.54," TR 32-542, Dec. 1963, Jet Propulsion Lab.

[11] Yates, C. L. and Rice, J. L., "Liquid Jet Penetration," *Research and Development Programs Quarterly Report*, U-RQR/69-2, April-June 1969, Applied Physics Lab., Johns Hopkins Univ.

FEBRUARY 1970 J. SPACECRAFT VOL. 7, NO. 2

# Applicability of Hypersonic Small-Disturbance Theory and Similitude to Internal Hypersonic Conical Flows

SANNU MÖLDER* AND NORBERT D'SOUZA†
*McGill University, Montreal, Canada*

**The applicability of hypersonic small-disturbance theory and its attendant hypersonic similitude to internal hypersonic flows is examined by comparing the exact conical flow solutions to their small-disturbance counterparts for 1) internal conical flow axisymmetric inlets with leading edge shock (ICFA) and 2) conical flow, Busemann-type axisymmetric inlets. The associated small-disturbance hypersonic similarity law is demonstrated for these internal flows. The results shown are for ideal gas flows in inlets with sharp leading edge. The surface pressures for Busemann inlet are compared with the available experimental data. A convenient method, based on hypersonic similitude, is presented for calculating Busemann-type inlet shapes.**

## Nomenclature

$C_p$ = pressure coefficient = $2(p - p_\infty)/\rho_\infty U_\infty^2$
$D$ = inlet diameter
$f$ = part of the stream function [See Eq. (6a)]
$j$ = constant which is zero for two-dimensional flow, unity for axially symmetric flow
$K$ = hypersonic similarity parameter
$l$ = length
$M$ = Mach number
$p$ = pressure
$r$ = radius in cylindrical or spherical coordinates
$R$ = characteristic inlet radius
$t$ = time
$T$ = temperature
$u,v$ = velocity components in cylindrical or spherical coordinates
$U$ = streamwise reference velocity
$x,r$ = Cartesian coordinates with $x$ in streamwise direction
$y$ = transverse distance measured from the streamwise axis through the leading edge
$\alpha$ = conical variable = $\tan^{-1}\sigma$
$\gamma$ = ratio of specific heats
$\delta$ = body deflection angle
$\theta$ = angle measured from $x$ axis
$\xi$ = nondimensional longitudinal distance
$\rho$ = density
$\sigma$ = conical variable = $\bar{r}/\bar{x}$
$\tau$ = body or shock slope
$\omega$ = entropy function
$\psi$ = stream function
$\zeta$ = see Eq. (10)
$\Gamma$ = see Eq. (17)

*Subscripts*

0 = refers to shock or leading edge
2,3 = upstream and downstream conditions for shock, respectively
$t, \infty$ = total and freestream conditions, respectively

*Superscripts*

$(\bar{\ })$ = dimensionless form
$(\ )'$ = derivative with respect to conical variable $\sigma$
$(\dot{\ })$ = derivative with respect to $\alpha$
$(\ )^*$ = value at the singular line

Received May 8, 1969; revision received August 6, 1969. This work has been financially supported by National Research Council Grant 4190.

* Associate Professor, Department of Mechanical Engineering. Member AIAA.

† Research Assistant and Commonwealth Scholar, Department of Mechanical Engineering.

## Introduction

THE hypersonic small-disturbance theory (HSDT) is based on the assumptions that the slope of the local surface of the body in the streamwise direction is everywhere small compared with unity; the velocity perturbations are small compared with the freestream velocity, and the pressure perturbations are small compared with the freestream dynamic pressure. However, the velocity perturbations are not small compared with the freestream sonic speed, and pressure perturbations are not small compared with the freestream static pressure.

The usefulness of HSDT and the resulting hypersonic similitude arises from the fact that the body or shock slope parameter, $\tau$, can be combined with the freestream Mach number, $M_\infty$, and the independent variables, thereby simplifying the basic conservation equations. This can be done for $\tau$ sufficiently small and $M_\infty\tau$ of the order unity. Hypersonic similitude arises directly from the HSDT. It relates flows past similarly shaped bodies at different $M_\infty$'s when $K = M_\infty\tau$ is kept constant, thus reducing the number of independent parameters by one.

Solution of the HSDT equations and the existence of the similarity law have been amply demonstrated for flow over wedges, cones and ogives.[1,2] Since the assumptions involved

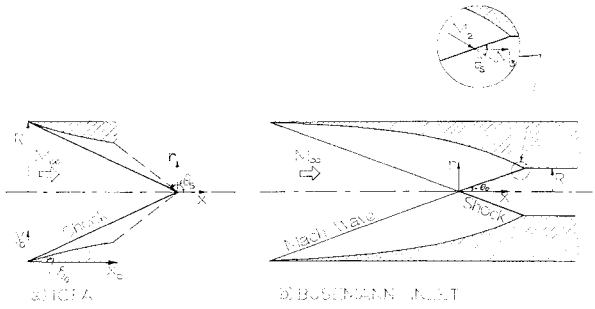

**Fig. 1 Internal conical flow, axisymmetric (ICFA) and Busemann-type internal conical flows.**

make use of large $M_\infty$ and small $\tau$, it is of interest to determine the lower limit on $M_\infty$ and upper limit on $\tau$ for which the similarity law is still applicable. This has been done for external flow over bodies,[2,3] but no such comparisons exist for internal flows. It is the purpose of this paper to find the region of applicability of the HSDT and to show the existence of hypersonic similitude for internal hypersonic flows. Since the loss of applicability (when proceeding towards low $M_\infty$ and high $\tau$) is gradual, a 5% discrepancy between the HSDT and the exact value of surface pressure coefficient has been used[3] as a criterion for applicability. In the comparisons of Ref. 3, the pressure on a cone or wedge surface is constant, so there is no difficulty in determining what to compare, whereas for internal flows, pressure varies along the surface, so that one must select distinct corresponding surface points and compare pressures at these points.

To verify the applicability of HSDT to internal flows we need to compare the solution obtained from the small-disturbance equations either to the solution obtained by a more exact method, or to experimental results. To facilitate comparison, we have considered conical flows, since the equations of motion and their small-disturbance versions reduce to the Taylor-Maccoll equation [Eq. (1), Ref. 4] and its small-disturbance version [Eq. (25), Ref. 1]. Solutions of each of these equations are then generated for two types of internal flows: 1) a uniform parallel stream which passes through a downstream-pointing conical shock and then converges towards the axis (ICFA; see Fig. 1a); and, 2) a uniform parallel stream which is compressed isentropically, then passes through a conical shock in such a way that the flow downstream of the shock is again uniform and parallel (Busemann inlet; Fig. 1b). These flows are discussed extensively in Ref. 4. Streamlines of the second flow can be used to construct a variety of hypersonic air inlets.[5,6] Some experimental results are available for this case as well. The restriction of conical and axial symmetry has no fundamental bearing on the HSDT assumptions, and thus there are no reasons to believe that deductions made under these restrictions should not have more general validity.

To demonstrate hypersonic similitude, we need to show that for a series of bodies, characterized by a body or shock slope parameter, $\tau$, where $M\tau$ is constant, the flow geometry and pressure distribution are the same for every member of the series provided the geometry and pressure are plotted against a distance that has been scaled with respect to $\tau$. We cannot use the HSDT to calculate the solution (e.g., the pressure distribution), because hypersonic similitude is an inherent part of HSDT, and we would be surprised indeed if use of HSDT did not yield perfect similitude. So, we must use the "exact" Taylor-Maccoll equation for ICFA and Busemann inlet flows in calculating the flow geometries (streamline shapes) and pressure distributions.

## Small-Disturbance Equations for Two-Dimensional and Axisymmetric Flows

The basic equations of motion expressing the conservation of mass, momentum and energy for two-dimensional or axisymmetric steady flows with independent coordinates $(x,r)$ may be written as

$$\partial(\rho u)/\partial x + \partial(\rho v)/\partial r + j\rho v/r = 0 \tag{1a}$$

$$u\partial u/\partial x + v\partial u/\partial r + (1/\rho)\partial p/\partial x = 0 \tag{1b}$$

$$u\partial v/\partial x + v\partial v/\partial r + (1/\rho)\partial p/\partial r = 0 \tag{1c}$$

$$u(\partial/\partial x)(p/\rho^\gamma) + v(\partial/\partial r)(p/\rho^\gamma) = 0 \tag{1d}$$

By normalizing with respect to $\tau$, we introduce new independent variables which are of the order unity throughout the flowfield.[1] The new variables are

$$\bar{x} = x; \quad \bar{r} = r/\tau; \quad \bar{u} = [(u/U_\infty) - 1]/\tau^2$$
$$\bar{v} = v/U_\infty\tau; \quad \bar{p} = p/p_\infty\gamma M_\infty{}^2\tau^2; \quad \bar{\rho} = \rho/\rho_\infty \tag{2}$$

Introducing these new barred variables in Eqs. (1) and neglecting the terms containing $\tau^2$ explicitly we obtain the first-order hypersonic small-disturbance equations:

$$\partial\bar{\rho}/\partial\bar{x} + \partial(\bar{\rho}\bar{v})/\partial\bar{r} + j\bar{\rho}\bar{v}/\bar{r} = 0 \tag{3a}$$

$$\partial\bar{v}/\partial\bar{x} + \bar{v}\partial\bar{v}/\partial\bar{r} + (1/\bar{\rho})\partial\bar{p}/\partial\bar{r} = 0 \tag{3b}$$

$$(\partial/\partial\bar{x})(\bar{p}/\bar{\rho}^\gamma) + \bar{v}(\partial/\partial\bar{r})(\bar{p}/\bar{\rho}^\gamma) = 0 \tag{3c}$$

A stream function $\psi(\bar{x},\bar{r})$ is introduced so that the continuity equation (3a) is identically satisfied. $\psi$ is defined such that

$$\partial\psi/\partial\bar{x} = -\bar{\rho}\bar{v}\bar{r}^j; \quad \partial\psi/\partial\bar{r} = \bar{\rho}\bar{r}^j \tag{4}$$

The small-disturbance equations in terms of the stream function become[1]

$$\left(\frac{\partial\psi}{\partial\bar{r}}\right)^2\left(\frac{\partial^2\psi}{\partial\bar{x}^2}\right) - 2\frac{\partial\psi}{\partial\bar{x}}\frac{\partial\psi}{\partial\bar{r}}\frac{\partial^2\psi}{\partial\bar{x}\partial\bar{r}} + \left(\frac{\partial\psi}{\partial\bar{x}}\right)^2\left(\frac{\partial^2\psi}{\partial\bar{r}^2}\right) =$$

$$\begin{cases} \left(\dfrac{\partial\psi}{\partial\bar{r}}\right)^{\gamma+1}\left[\gamma\bar{\omega}\dfrac{\partial^2\psi}{\partial\bar{r}^2} + \dfrac{d\bar{\omega}}{d\psi}\left(\dfrac{\partial\psi}{\partial\bar{r}}\right)^2\right] & \text{(5a)} \\ \text{for two-dimensional flow} \\ \dfrac{(\partial\psi/\partial\bar{r})^{\gamma+1}}{(\bar{r})^{\gamma-1}}\left[\gamma\bar{\omega}\left(\dfrac{\partial^2\psi}{\partial\bar{r}^2} - \dfrac{1}{\bar{r}}\dfrac{\partial\psi}{\partial\bar{r}}\right) + \dfrac{d\bar{\omega}}{d\psi}\left(\dfrac{\partial\psi}{\partial\bar{r}}\right)^2\right] & \text{(5b)} \\ \text{for axisymmetric flow} \end{cases}$$

where $\bar{\omega}(\psi) = \bar{p}/\bar{\rho}^\gamma$ = entropy function.

## Hypersonic Small-Disturbance Theory Applied to Flows with Conical Symmetry

Conical symmetry implies that flow variables do not change with respect to the radial coordinate. The stream function then takes the form

$$\psi(\bar{x},\bar{r}) = \bar{x}^{j+1}f(\sigma) \tag{6a}$$

where $\sigma$ is a conical variable defined by

$$\sigma = \bar{r}/\bar{x} = \tan\theta/\tau \tag{6b}$$

Introducing this transformation in Eqs. (5), and noting that the entropy field is uniform before the shock and again after the shock, the small-disturbance equation for axisymmetric conical flow reduces to

$$f'' = f'^2[2f - \gamma\bar{\omega}_s(f'/\sigma)^\gamma]/[4f^2 - \gamma\bar{\omega}_s(f'/\sigma)^{\gamma-1}f'^2] \tag{7}$$

where $\bar{\omega}_s = (\bar{p}/\bar{\rho}^\gamma)_s$ = entropy function at the shock; $f' = df/d\sigma$, and $f'' = d^2f/d\sigma^2$. This is the small-disturbance version of the Taylor-Maccoll equation. It is not a very popular equation because, just as the Taylor-Maccoll equation, it requires a numerical solution, and, furthermore, it lacks the exactness of the latter. In our case, we find it useful, however, to compare solutions of Eq. (7) against the more exact Taylor-Maccoll equation with the aim of drawing parallel conclusions about the accuracy of the more general Eqs. (5).

**Conical Axisymmetric Flow Behind an Inverted Shock**

The exact Taylor-Maccoll equation for axisymmetric conical flow is [Eq. (1), Ref. 4]

$$u'^2_r(u_r + u''_r) = (\gamma - 1)(1 - u_r^2 - u'^2_r) \times (u''_r + u'_r \cot\theta + 2u_r)/2 \quad (8a)$$

where $u_r$ is the velocity in the radial direction and

$$u_\theta = u'_r = du_r/d\theta \quad (8b)$$

is the velocity in the $\theta$ direction with $\theta$ measured from the freestream direction. Both velocities are nondimensionalized with respect to the maximum speed obtainable by expanding to zero absolute temperature. The solution obtained by this equation for ICFA is discussed in Ref. 4. It is interesting to note that the numerical solution, in passing downstream from the shock wave, reaches an impasse in the form of a singularity. The physical occurrence and implication of this singularity are not yet clearly understood. However, for our purposes here, we have found that the same singularity also occurs in the small-disturbance version of the Taylor-Maccoll equation [Eq. (7)], so that it is reasonable to compare the two solutions at the singularity, especially when it is realised that this is the point of highest contraction, and this is, after all, the aspect we are interested in, insofar as it influences the small-disturbance theory.

Referring to Fig. 1a, we define the parameter $\tau$ in terms of the slope of the shock wave, $\tau_s = |\tan\theta_s|$, where $\theta_s$ is the shock angle. We define a similarity parameter, $K_s = M_\infty\tau_s$. The boundary conditions at the shock surface are obtained from the oblique shock relations and may be simplified to[1]

$$\sigma_s = -1, f_s = \tfrac{1}{2}, f'_s = [(\gamma + 1)K_s^2/\{2 + (\gamma - 1)K_s^2\}]\sigma_s$$

and

$$\bar{\omega}_s = \left[\frac{2\gamma K_s^2 - (\gamma - 1)}{\gamma(\gamma + 1)K_s^2}\right]\left[\frac{2 + (\gamma - 1)K_s^2}{(\gamma + 1)K_s^2}\right]^\gamma \quad (9)$$

Since we have defined the independent variable, $\sigma = (\tan\theta)/\tau_s$, we note that when $\theta = \pi/2$, $\sigma$ becomes $\pm\infty$, and there will be a difficulty in choosing a step size for the numerical solution in this region. Therefore, we introduce a new independent variable, $\alpha \equiv \tan^{-1}\sigma$, which decreases smoothly from $\frac{3}{4}\pi$ at the shock surface to zero at the axis. Equation (7) becomes

$$\ddot{f} = 2\dot{f}\tan\alpha + [\dot{f}^2(2f - \gamma\bar{\omega}_s\zeta^\gamma)/(4f^2 - \gamma\bar{\omega}_s\tan^2\alpha\,\zeta^{\gamma+1})] \quad (10)$$

where $\dot{f} = df/d\alpha$, $\ddot{f} = d^2f/d\alpha^2$, and $\zeta = \dot{f}/(\tan\alpha)(1 + \tan^2\alpha)$.

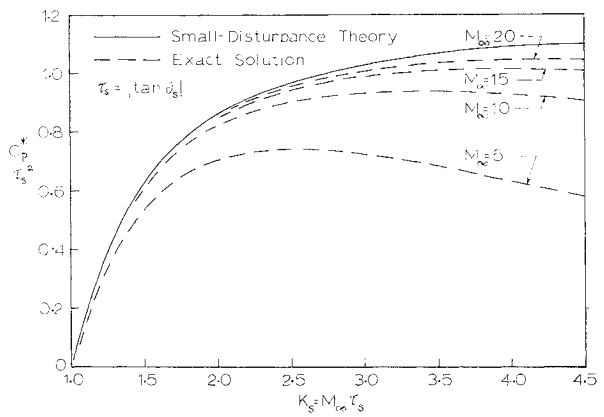


**Fig. 2 Variation of pressure coefficient at singular line with $K_s$ for ICFA.**

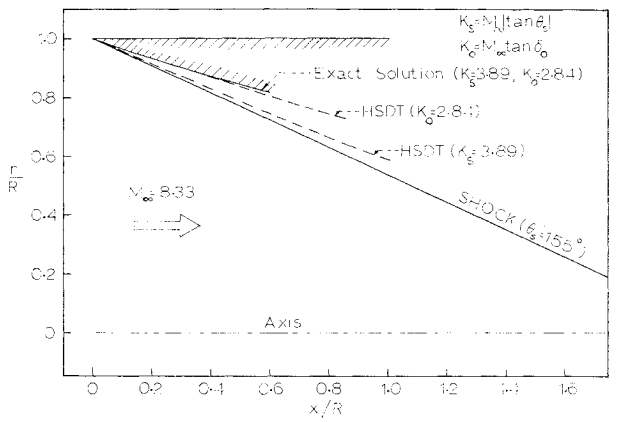


**Fig. 3 Streamline shape of ICFA, calculated from the hypersonic small-disturbance theory (HSDT) and the exact Taylor-Maccoll equation.**

The boundary conditions at the shock surface become

$$\alpha_s = 3\pi/4, f_s = \tfrac{1}{2}; \quad \dot{f}_s = -2(\gamma + 1)K_s^2/[2 + (\gamma - 1)K_s^2] \quad (11)$$

Equation (10) with the boundary conditions given by Eq. (11) is solved on a digital computer. Once the solution $f$, $\dot{f}$, and $\ddot{f}$ is obtained with respect to the independent variable $\alpha$, the following additional quantities can be found

$$\sigma = \tan\alpha, f' = \dot{f}/(1 + \sigma^2), f'' = (\ddot{f} - 2\sigma\dot{f})/(1 + \sigma^2)^2$$
$$\bar{\rho} = f'/\sigma, \bar{p} = \bar{\omega}_s\bar{\rho}^\gamma, \bar{v} = \sigma - 2f/f' \quad (12)$$
$$\bar{u} = 1/(\gamma - 1)K_s^2 - [\gamma/(\gamma - 1)]\bar{p}/\bar{\rho} - \bar{v}^2/2$$

The results obtained are compared with the exact solution obtained from the Taylor-Maccoll equation [Eq. (8a)]. For the purpose of comparison, the surface pressure coefficients at the singular lines[4] for various $M_\infty$'s are obtained for different values of $K_s$ (Fig. 2).

The stream-line shapes obtained by the HSDT and the Taylor-Maccoll equation are compared in Fig. 3. The range of HSDT applicability to the ICFA inlet, wherein the surface pressure coefficients at the singular line deviate 5% from the limiting value, is shown in Fig. 4. This boundary in fact, gives the lower limit on $M_\infty$ and upper limit on $\tau_s$, for which the results obtained from the small-disturbance equations are within 5% of the exact solution.

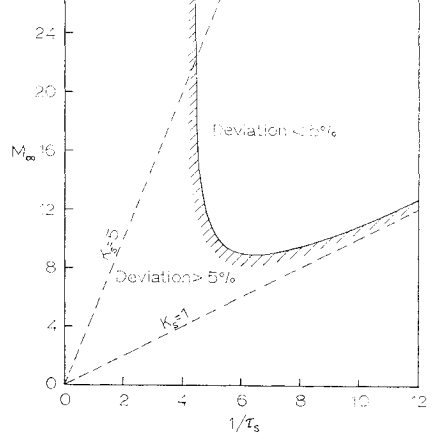


**Fig. 4 Range of applicability of HSDT for ICFA.**

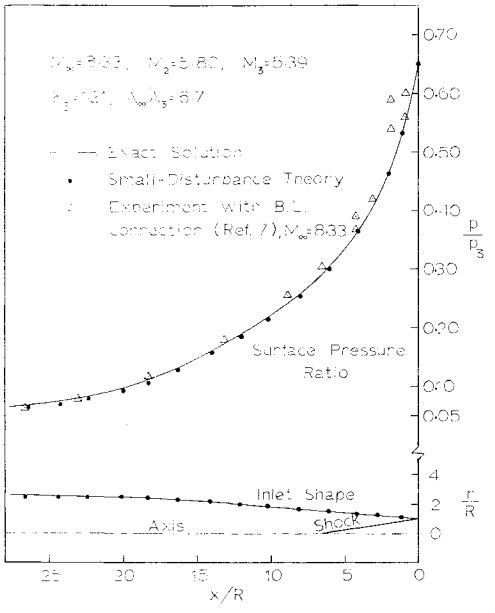


**Fig. 5 Surface pressure distributions obtained from HSDT, the exact Taylor-Maccoll equation, and from experiments for Busemann inlet.**

### Axisymmetric Busemann Inlet

For the Busemann inlet, the downstream flow conditions behind the shock, $M_3$ and $\theta_0$ (Fig. 1b), are taken as reference conditions. The small-disturbance parameters are defined as

$$\tau_0 = \tan\theta_0,\ K_0 = M_3\tau_0,\ \sigma = \tan\theta/\tau_0 \tag{13}$$

and the small-disturbance variables [Eqs. (2)], normalized in terms of the reference conditions become

$$\bar{x} = x;\quad \bar{r} = r/\tau_0;\quad \bar{u} = [(u/U_3) - 1]/\tau_0^2$$
$$\bar{v} = v/U_3\tau_0;\quad \bar{p} = p/p_3\gamma M_3^2\tau_0^2;\quad \bar{\rho} = \rho/\rho_3 \tag{14}$$

Since it is convenient to obtain the flow conditions across the shock by specifying $M_2$ immediately upstream of the shock and $\theta_s$ (Fig. 1b), we define the similarity parameter $K_s$ as:

$$K_s = M_2 \sin\theta_s \tag{15a}$$

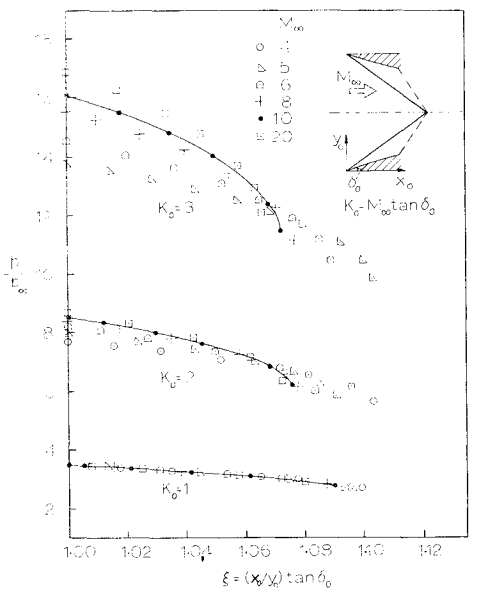


**Fig. 6 Surface pressure ratio vs the length parameter for various values of the hypersonic similarity parameter, $K_0$, for ICFA.**

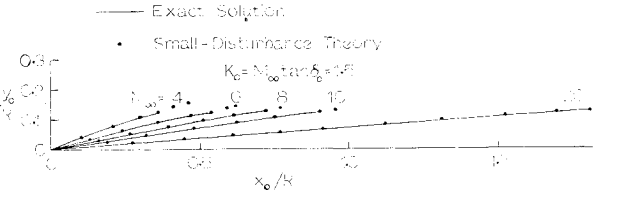


**Fig. 7 Affinely related inlet shapes for ICFA (see Fig. 1a).**

Then,

$$K_0 = \{[(\gamma - 1)K_s^2 + 2]/[2\gamma K_s^2 - (\gamma - 1)]\}^{1/2} \tag{15b}$$

The small-disturbance Eq. (10) is integrated in the upstream direction starting from the shock surface. The boundary conditions at the shock are as follows: $\sigma_0 = 1$, $\alpha_0 = \pi/4$, $f_0 = \bar{p}_0(1 - \bar{v}_0)/2$, and $f_0' = 2\bar{p}_0$, where $\bar{v}_0$ and $\bar{p}_0$ are calculated from the oblique shock relations.

In integrating Eq. (10), when $\alpha = \pi/2$, $\tan\alpha$ becomes infinite and in this region the following simplified equation applies:

$$f'^2 - 2ff'' = 0 \tag{16}$$

Equation (16) is substituted instead of Eq. (10) in the region where $\alpha \to \pi/2$, to carry out the numerical integration. The flow variables $\bar{p}$, $\bar{\rho}$, $\bar{v}$, and $\bar{u}$ are obtained from Eqs. (12).

The streamline shape and the surface pressure distribution, as obtained from the solution of Eq. (10), are compared with the exact solution obtained from the Taylor-Maccoll equation in Fig. 5. For this particular case, $M_\infty = 8.33$, $\theta_s = 12.05°$, the flow turning angle is 3.132°, and $M_3 = 5.39$. This inlet has a theoretical total pressure recovery of 0.99 and an area ratio of 6.7. Agreement between the HSDT and exact solutions is good. The experimental pressure distribution, obtained for this inlet with correction for the effects of the laminar boundary-layer displacement thickness,[7] based on an adaptation of Tani's method to compressible flow, is shown in Fig. 5. There is good agreement between the calculated and measured surface pressure values.

## Applicability of Similarity Law to Hypersonic Internal Flows

The application of HSDT to internal flows leads to the conclusion that the similarity law,[2,8] which connects flows at different Mach numbers past related shapes, should apply to hypersonic internal flows. Let us first use the results obtained from the solution of Taylor-Maccoll equation to demonstrate the applicability of similarity law to ICFA.

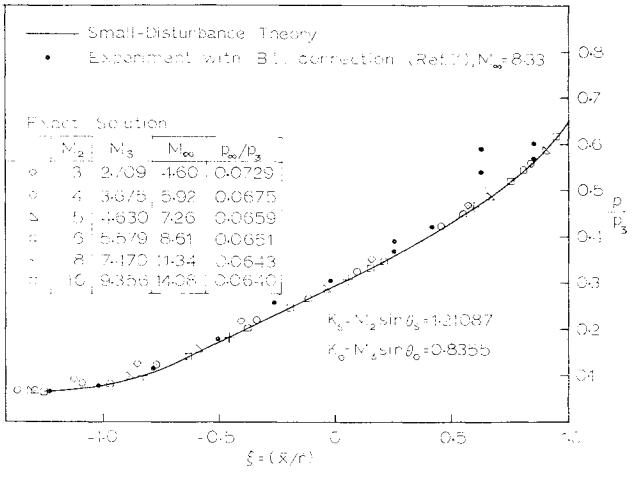


**Fig. 8 Variation of pressure ratio along the Busemann inlet (see Fig. 1b) for a constant value of similarity parameter at different Mach numbers.**

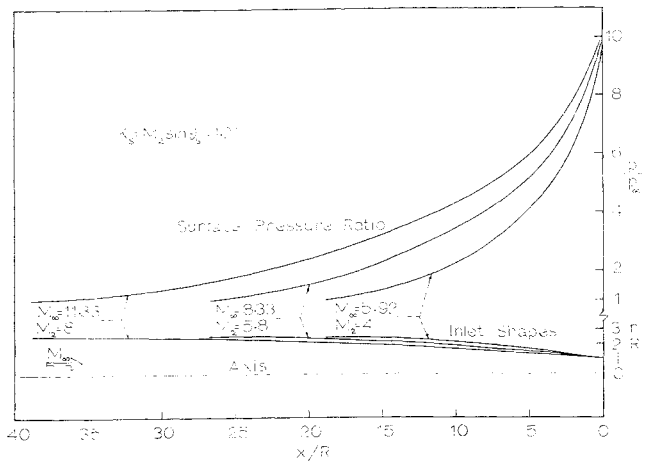


**Fig. 9 Busemann inlet streamline shapes and surface pressure distributions for various $M_\infty$'s for a given similarity parameter, $K_s$.**

The hypersonic similarity parameter is defined in terms of the body slope at the leading edge, $K_0 = M_\infty \tan\delta_0$. The static pressure ratio is plotted against the longitudinal non-dimensional distance $\xi = (x_0/y_0)\tan\delta_0$ in Fig. 6. The hypersonic similitude is applicable to these inlets for $K_0 \leq 2.0$. The affinely related inlet shapes for $K_0 = 1.5$ are shown in Fig. 7.

Now let us use the results obtained from the solution of the exact Taylor-Maccoll equation to demonstrate the applicability of the similarity law to Busemann inlet. The surface pressure distribution is plotted at related distances expressed in terms of a non-dimensional parameter $\xi = \bar{x}/\bar{r} = \tau_0/\tan\theta$. Figure 8 gives the pressure distribution along the surface of the Busemann inlet for a constant value of $K_s = M_2 \sin\theta_s = 1.21087$, with $M_2$ and $\theta_s$ taking on various values. The HSDT result is shown as a solid line; it corresponds very well to the more accurate exact calculations. The percentage error increases towards the entrance of the inlet.

Figure 8 demonstrates that the hypersonic similarity law is applicable to Busemann inlets. The affinely related shapes and the corresponding pressure distributions for the same value of $K_s$, are shown in Fig. 9. This figure shows, in effect, the shape changes required to maintain a constant efficiency and constant area-ratio inlet which produces a uniform and parallel exit stream.

Figure 10 gives surface pressure ratio vs $\xi$ for a series of $K_s$ values. The range of applicability of hypersonic similarity law to Busemann inlet is shown in Figs. 11 and 12.

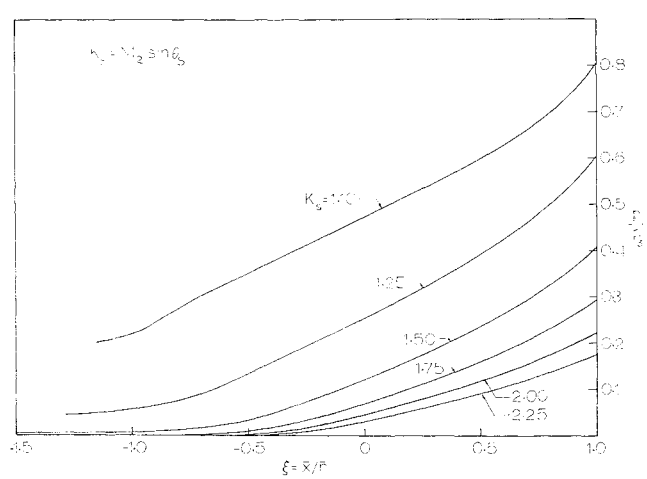


**Fig. 10 Variations of pressure ratio along Busemann inlet for different values of $K_s$.**

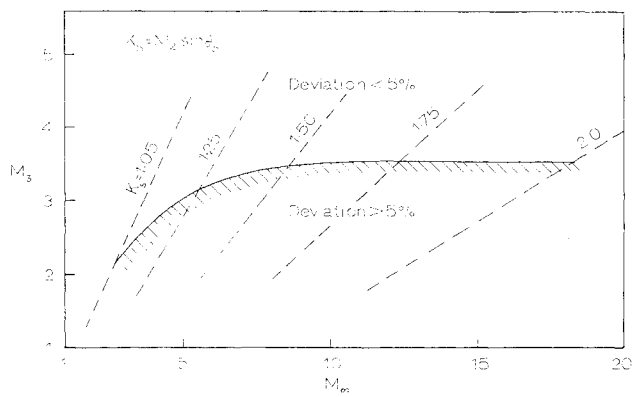


**Fig. 11 Range of applicability of similarity law for Busemann inlet.**

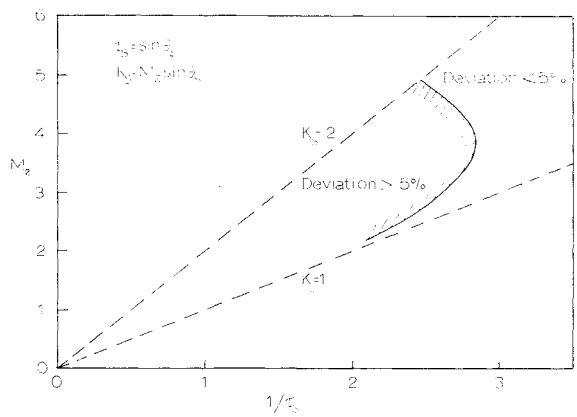


**Fig. 12 Range of applicability of similarity law for Busemann inlet.**

Our criterion for hypersonic similarity here is that the exact value of the surface pressure ratio at $\xi = 0$ should not differ by more than 5% from its limiting value. Figure 11 shows that the HSDT and the associated hypersonic similitude will hold for $M_3 \geq 3.5$. It is convenient to start calculations for Busemann-type inlets by specifying $\theta_s$ and $M_2$ because the usual freestream starting point at the leading edge has a smooth singularity in the Taylor-Maccoll equations. Figure 12 shows that HSDT holds to 5% as long as $1/\sin\theta_s \geq 2.85$, (or $\theta_s \leq 20°$), for all values of $M_2$.

The surface contours of Busemann inlets calculated by the HSDT are unique for each value of $K_s$ (Fig. 13). Suppose we are given $M_\infty$ and a desired total pressure recovery, $P_{t_3}/P_{t_\infty} = 0.93$. To find the shape of a Busemann inlet rapidly, one would proceed as follows. From Fig. 14, we find that $P_{t_3}/P_{t_\infty} = 0.93$ corresponds to $K_s = 1.50$, which corresponds to $D_\infty/D_3 = 6.7$. Knowing $M_\infty$ and $K_s$ from Fig. 15, we get $M_3$. We calculate $K_0$ from Eq. (15b) then, $\theta_0 = \sin^{-1}(K_0/M_3)$. $M_2$ is obtained from Fig. 15, then $\theta_s = \sin^{-1}(K_s/M_2)$.

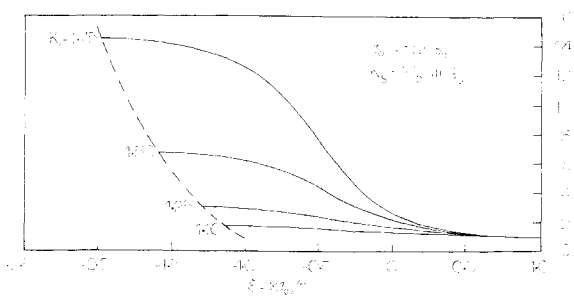

**Fig. 13 Streamline shapes for Busemann inlet at different values of similarity parameter, $K_s$.**

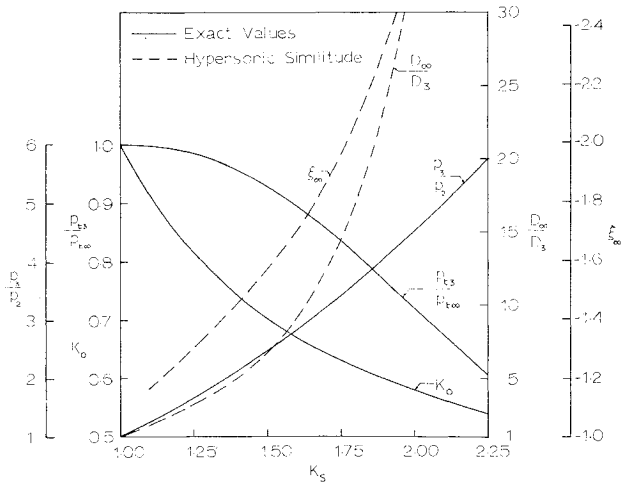


**Fig. 14 Variation of design parameters with $K_s$ for Busemann inlet.**

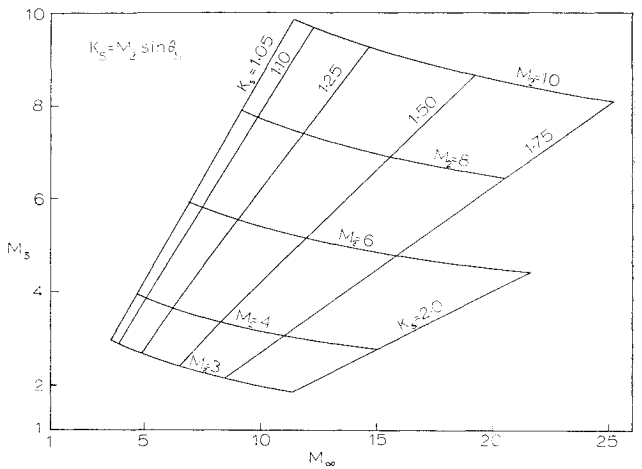


**Fig. 15 Variation of diffused Mach number with free-stream Mach number for Busemann inlet.**

We calculate

$$p_3/p_\infty = (\Gamma_\infty/\Gamma_2)^{\gamma/(\gamma-1)}[2\gamma K_s^2 - (\gamma - 1)]/(\gamma + 1)$$

$$T_3/T_\infty = (\Gamma_\infty/\Gamma_2)[2\gamma K_s^2 - (\gamma - 1)] \times [(\gamma - 1)K_s^2 + 2]/[(\gamma + 1)^2 K_s^2] \quad (17)$$

where $\Gamma_i = 1 + (\gamma - 1)M_i^2/2, i = \infty$ or 2. With the known value of $\tau_0$ the inlet shape is obtained from Fig. 13.

## Conclusions

1) The hypersonic small-disturbance theory (HSDT) has been applied to internal axisymmetric conical flows, and it has been demonstrated that a 5% accuracy in surface pressure can be obtained for ICFA as long as the similarity parameter $K_s = M_\infty \tau_s$ exceeds 1.0 and $1/\tau_s$ exceeds 4.5; and for Busemann inlet flow as long as the diffused Mach number $M_3$ exceeds 3.5 or $1/\tau_s$ exceeds 2.85. The HSDT solution represents the limiting solution of the exact equations and may be used to obtain the flow parameters with reasonable accuracy in any hypersonic internal flow, as long as the assumptions of HSDT are not violated.

2) Hypersonic similitude is demonstrated for both ICFA and Busemann-type internal flows; the surface pressure curves and streamline shapes are similar when plotted against the nondimensional longitudinal distance $\xi$ for internal flows with same values of similarity parameter. This will be useful in correlating existing data and in the determination of flow properties in a family of internal flows, (e.g., inlets with sharp leading edges), where this law is expected to apply.

3) A convenient method, which uses hypersonic similitude, is presented for calculating Busemann-type inlet shapes. Required geometry variation is presented for an inlet which is to maintain constant values of area ratio and total pressure recovery. Similar method may be used for other types of hypersonic internal flows where hypersonic similitude is applicable.

## References

[1] Van Dyke, M. D., "A Study of Hypersonic Small-Disturbance Theory," Rept. 1194, 1954, NACA.

[2] Ehret, D. M., Rossow, V. J., and Stevens, V. I., "An Analysis of the Applicability of the Hypersonic Similarity Law to the Study of Flow about Bodies of Revolution at Zero Angle of Attack," TN, 2250, Dec. 1950, NACA.

[3] Chernyi, G. G., *Introduction to Hypersonic Flow*, Academic Press, New York, 1961, Chap. II.

[4] Mölder, S., "Internal, Axisymmetric Conical Flow," *AIAA Journal*, Vol. 5, No. 7, July 1967, pp. 1252–1255.

[5] Mölder, S. and Szpiro, E. J., "Busemann Inlet for Hypersonic Speeds," *Journal of Spacecraft and Rockets*, Vol. 3, No. 8, Aug. 1966, pp. 1303–1304.

[6] Mölder, S., *Aerodynamic Performance and Geometric Contours for Hypersonic Inlets of the Busemann Type*," 1968; obtainable from the author: Dept. of Mechanical Engineering, McGill Univ., Montreal.

[7] Mölder, S. and Romeskie, J. M., "Modular Hypersonic Inlets with Conical Flow," *AGARD Conference Proceedings No. 30, Hypersonic Boundary Layers and Flow Fields*, May 1968.

[8] Hayes, W. D. and Probstein, R. F., *Hypersonic Flow Theory*, Vol. 1, Inviscid Flows, Academic Press, New York, 1966, Chap. II.